Method for calculating non-stationary heat flux from a sensor signal on heterogeneous metal structures

© P.A. Popov

Ioffe Institute, St. Petersburg, Russia
E-mail: pavel.popov@mail.ioffe.ru

Received May 3, 2024
Revised July 1, 2024
Accepted October 30, 2024

Numerical simulation of non-stationary thermal and thermoelectric processes in a sensor on a heterogeneous structure of a copper–nickel pair for conditions behind a reflected shock wave and external supersonic flow around the body is carried out. Good agreement between electrical signals, volt-watt coefficient obtained in calculation and experiment is obtained. The heat flux calculated using the proposed method is close to the theoretical value.

Keywords: sensor, shock tube, heat flux, measurement.

DOI: 10.61011/TPL.2024.12.60346.6604k

The diagnostics of heat flux to the surface of a body with a supersonic gas flow around it is one of the key objectives in modern experimental gas dynamics. Of principal interest are the regimes with high enthalpy, when the properties of a real gas manifest themselves and dissociation and ionization reactions are initiated in the shock layer [1]. In a ground experiment, such conditions may be established only at pulsed-operation facilities [2]. Therefore, the used heat flux sensors should have a fast response ($\sim 10\,\mu$s at a measurement duration of ~ 10 ms), a wide dynamic range (from ~ 100 kW/m^2 to ~ 10 MW/m^2), and a sufficient mechanical strength.

Coaxial thermocouples [3] are the basic heat flux sensors at high-enthalpy facilities. They offer a sufficient performance and an acceptable mechanical strength. It is known from experience that the force impact of a gas flow and diaphragm particles may lead to loss of electrical contact on the working surface and necessitate monitoring of their condition and periodic test calibration. This is the reason why other types of sensors with increased mechanical strength are being developed actively at present [4].

A heat flux sensor based on heterogeneous metal structures (heterogeneous gradient heat flux sensor, HGHFS) designed at Peter the Great St. Petersburg Polytechnic University complies fully with these requirements [5]. The sensitive element of the HGHFS is a plate made of alternating layers of copper and nickel oriented at a certain angle to the working surface. The layers are coupled by diffusion welding, which ensures high mechanical strength of the resulting structure and constancy of the sensor parameters in experiments. The leads for connection to the recording system are welded to the side faces of the plate. The sensor is glued flush with the surface of the model. The gap between the side faces of the plate and the body of the model is filled with acrylic. Particular attention is paid to the quality of thermal contact on the back surface, since its loss may lead to a noticeable distortion of the temperature field and the electrical signal in long-term measurements (~ 1 ms). The HGHFS operating principle consists in generation of a seebeck coefficient in a structure with anisotropy of the thermoelectric coefficient when a temperature gradient is established in it [6].

The key element governing the reliability and accuracy of measurements of non-stationary heat fluxes is the method for calculation of the heat flux based on the electrical sensor signal, which should incorporate a valid thermal and thermoelectric model. The main objective of the present study is to analyze thermal and thermoelectric processes in the HGHFS under various heating conditions typical of experiments in shock tubes and to test the method for calculating the heat flux based on the electrical sensor signal.

The study was conducted in two stages. The direct problem was solved at the first stage. Heat flux q_h passing through the working surface of the sensor was set, and system of equations

$$C\rho\frac{\partial T}{\partial t} = \mathrm{div}\mathbf{q},$$

$$\mathrm{div}\mathbf{j} = 0 \qquad (1)$$

was solved numerically to determine the distribution of temperature $T(t, x, y)$ and electrical potential $\varphi(t, x, y)$ with account for the layered structure. Here, $\mathbf{q} = -\lambda\nabla T$ and $\mathbf{j} = -\sigma\nabla\varphi - \sigma\alpha\nabla T$ are the densities of the heat flux and the electric current; λ, σ, and α are the thermal conductivity, electrical conductivity, and Seebeck coefficients. Thermal and electrical insulation conditions were set on the side faces. Thermal EMF $\Delta\varphi(t)$ was recorded between the extreme points on working $y = h$ and back $y = 0$ surfaces, between side faces $x = 0$ and $x = l$, and also as the difference between the maximum and minimum values for the entire sensor. This choice was due to the uncertainty of positioning of the points of wire connection on the side faces of sensors from different batches, which is attributable to the specifics of their manufacture. A preliminary stationary calculation was carried out to determine volt–watt

Volt–watt coefficients (in μV/W) of a sensor $2.7 \times 2.7 \times 0.57$ mm in size obtained in calculations for a stationary thermal regime and in the experiment with calibration against a reflected shock wave

Maximum value	Working surface	Back surface	Vertical faces	Experiment
15.8	12.8	12.9	12.9	16

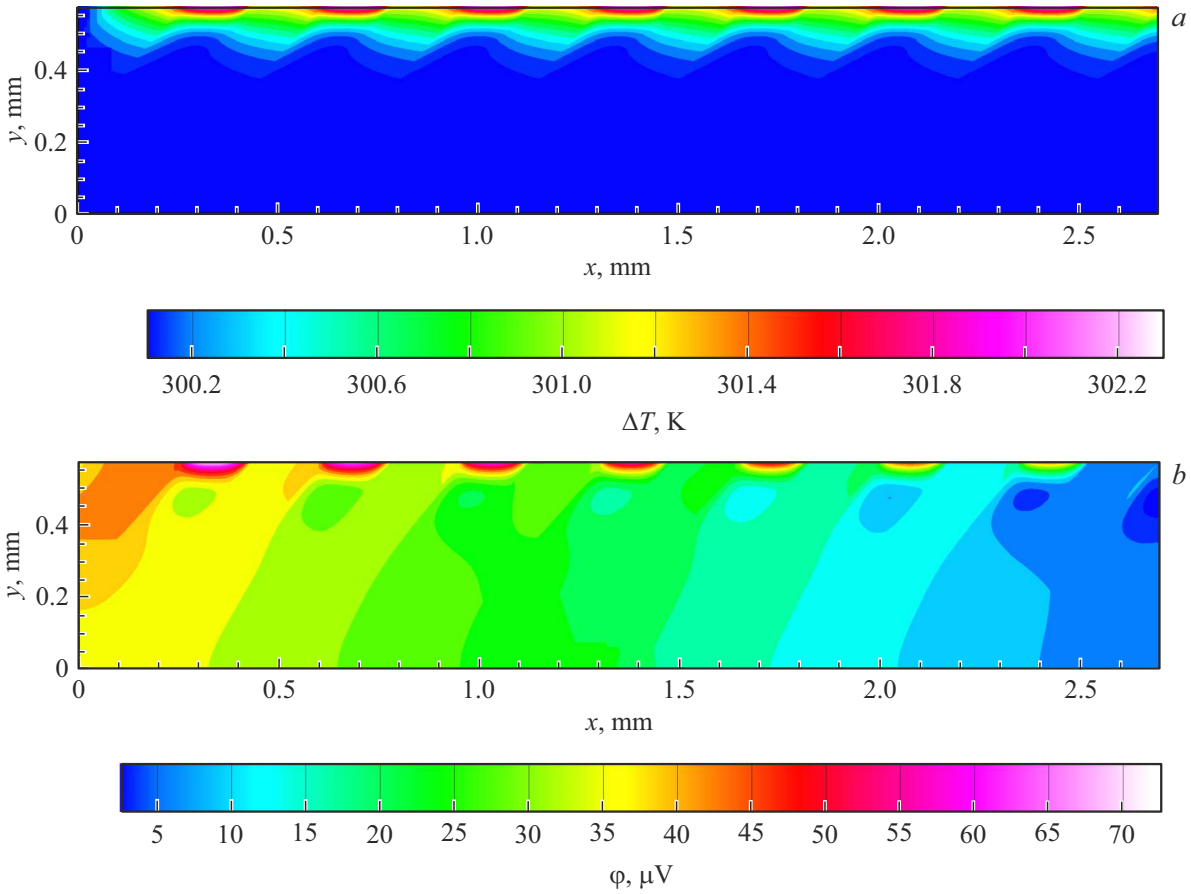

Figure 1. Temperature (a) and electrical potential (b) field at time moment $t = 50\,\mu$s for a sensor $2.7 \times 2.7 \times 0.57$ mm in size heated by gas behind a reflected shock wave with normalized heat flux $q_h\sqrt{t} = 26.5\,\text{kW} \cdot \sqrt{\text{s}}/\text{m}^2$.

coefficient $S_0 = \Delta\varphi/q_h A$, where A is the area and $\Delta\varphi$ is the electrical signal. Two heating regimes were then considered: heating by stationary gas behind a reflected shock wave with a characteristic process time of 1 μs and external supersonic gas flow around a blunt body with a characteristic time of 1 ms.

At the second stage, the inverse problem was solved: an approximate calculation of heat flux $q_h(t)$ based on $\Delta\varphi(t)$ and S_0 obtained at the first stage was performed. The approximation of a homogeneous medium with effective properties and a one-dimensional thermal and thermoelectric model were used. The model assumes that the length-to-thickness ratio is sufficiently large, side effects are negligible, and the primary contribution to the electrical signal is produced by the longitudinal thermal EMF component. Under these assumptions, the temperature difference between the working and back surfaces of the sensor is related to the electrical signal in the following way [7]:

$$\left[T_h(t) - T_0(t)\right] = \frac{h\Delta\varphi}{S_0\lambda_y A}, \tag{2}$$

where λ_y is the effective thermal conductivity of the multilayer structure in the vertical direction and h is the sensor height. Heat flux q_h was calculated by solving numerically the one-dimensional non-stationary thermal conductivity equation with a boundary condition of the first kind on the working surface (2). Dependence (2) is specific in that it features an unknown back surface temperature $T_0(t)$. In the method used, it is determined in the course of data processing. The thermal conductivity equation is solved cyclically for this purpose; temperature $T_0(t)$ at each

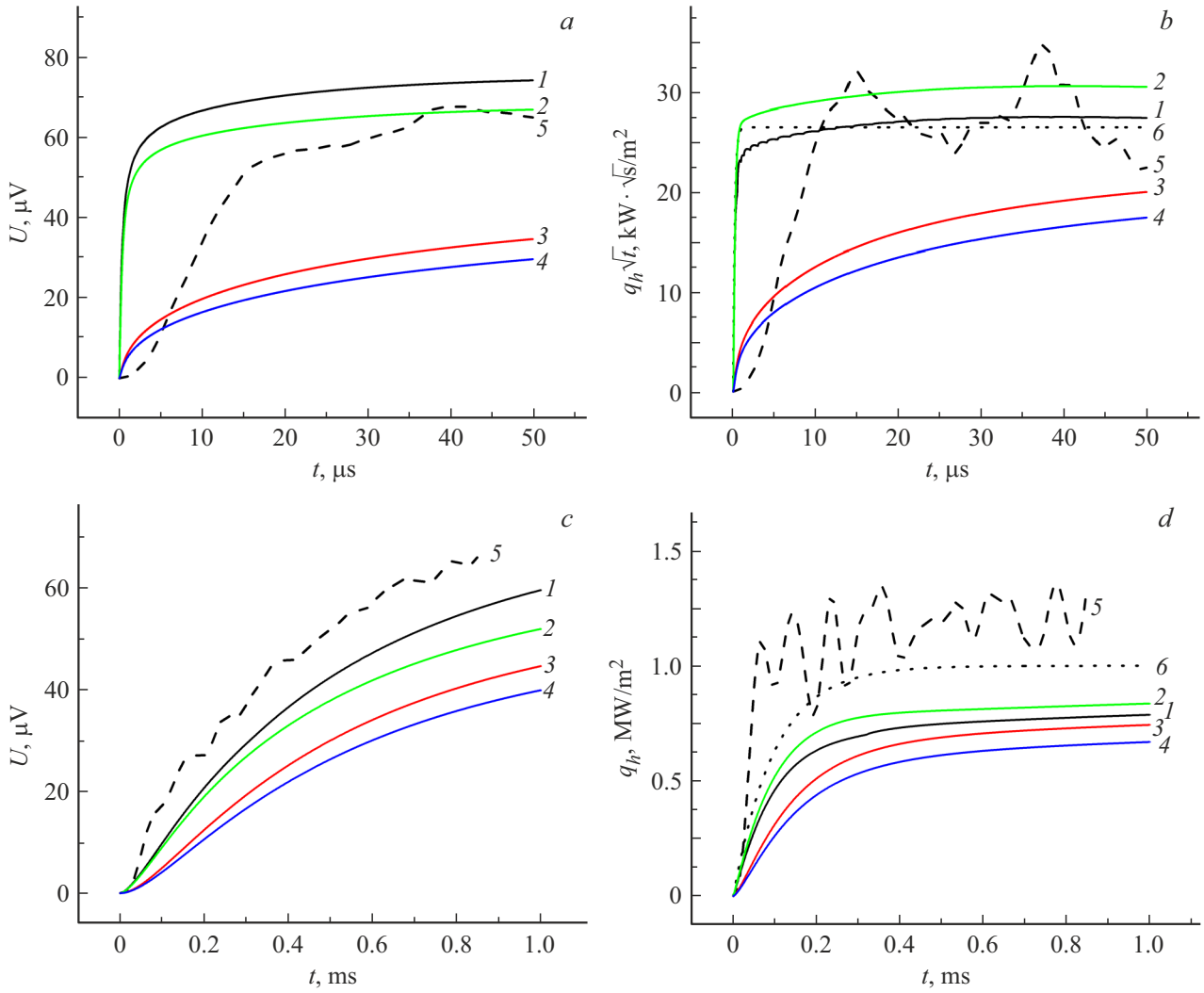

Figure 2. Electrical signals (a, c) and calculated heat flux (b, d) under sensor heating by gas behind a reflected shock wave (a, b) and at the critical point of a blunt body with a supersonic flow around it (c, d). *1* — Maximum signal, *2* — along the working surface, *3* — between vertical faces, *4* — along the back surface, *5* — experiment, and *6* — boundary condition.

moment in time is taken from the previous iteration:

$$T_h^{i+1}(t) = \frac{h}{S_0\lambda_y A}\Delta\varphi(t) + T_0^i(t). \qquad (3)$$

Condition $T_0^0(t) = 0$ is used as an initial approximation. This algorithm is convergent, since the change in $T_0(t)$ is small compared to the change in $T_h(t)$ under the conditions corresponding to experiments at pulsed gas-dynamic facilities. The experience to date has been that several iterations are sufficient to fulfill condition $|T_h^{i+1}(t) - T_h^i(t)| < 10^{-3}$ K in the case of a sensor with $h \approx 0.5$ mm and a measurement duration of ~ 1 ms.

The volt–watt coefficients for a sensor $2.7 \times 2.7 \times 0.57$ mm in size calculated for the stationary thermal regime are listed in the table. The experimental value was obtained with the use of calibration against a reflected shock wave [8]. The initial argon pressure in the driven section was $p_1 = 26.7$ kPa, and the Mach number of an incident shock wave was $M_1 = 3.86$. The electrical signal was processed using the method under study. The maximum deviation of calculated values from the experimental ones does not exceed 20%. Thus, it can be argued that two-dimensional model (1) characterizes the distribution of temperature and electrical potential correctly, and one-dimensional model (2) takes into account the key thermal and thermoelectric processes in the layered HGHFS structure.

Non-stationary temperature and electrical potential fields were calculated for the conditions of the calibration experiment described above. The normalized heat flux calculated based on the initial gas pressure in the driven section and the Mach number of an incident wave was $q_h\sqrt{t} = 26.5\,\text{kW} \cdot \sqrt{\text{s}}/\text{m}^2$. Figure 1 presents the calculation results at time moment $t = 50\,\mu$s. Since the thermal diffusivity of copper ($1.1 \cdot 10^{-4}$ m^2/s) and nickel ($2.3 \cdot 10^{-5}$ m^2/s) differ, isotherms have kinks, and the depth of heating in

nickel layers is noticeably smaller. This leads into different distributions of the temperature gradient along each layer and, accordingly, different thermoelectric field strengths $\mathbf{E}^T = -\alpha\nabla T$ [6]. Although isopotential lines concentrate in the region of maximum temperature gradients, they are parallel to the layer boundaries in the bulk of the sensor. It can be seen that the potential difference between the side faces is significantly greater than the one between the working and back surfaces. This is the principal condition of applicability of one-dimensional thermal and thermoelectric model (2). In the case of longer heating, typical for external flow around the body, the sensor is heated completely, and all isotherms become similar and have almost the same slope. Since there are no regions of maximum temperature gradients, equipotential lines have the same slope. This structure of the electric field is more consistent with the assumptions of model (2), which is reflected in the accuracy of calculation of the heat flux based on the electrical sensor signal.

The calculated electrical signals at various recording points are represented by solid curves in Fig. 2, *a*. The noticeable difference between curves *1*, *2* and curves *3*, *4* is attributable to the thermal EMF generation in local regions of maximum temperature gradients and to a substantially non-one-dimensional temperature field near the working surface. The dashed curve represents the experimental signal. The lack of a pronounced edge is due to the use of a $\times 500$ amplifier with an *RC* low-pass filter with a time constant of $5\,\mu$s. If follows from the comparison of calculated and experimental curves that the electrical signal in a real sensor is likely to be recorded approximately at the center of the side surfaces. Figure 2, *b* presents the solution of the inverse problem: the heat flux calculated based on the sensor signal. The corresponding volt–watt coefficient value (see the table) was used in each scenario. A noticeable difference in signals at different recording points leads into a proportional difference in heat fluxes. Oscillations of normalized heat flux $q_h\sqrt{t}$ obtained in the experiment are caused by noise due to a low signal level ($\sim 10\,\mu$V) and do not reflect the real gas-dynamic flow pattern. Despite these oscillations, its average value agrees closely with the maximum one and the one calculated along the working surface.

Figure 2, *c* shows the calculated and experimental electrical signals in the case of heating of a sensor $2.9 \times 2.9 \times 0.5$ mm in size mounted at the critical point of a blunt body 35 mm in radius with a supersonic gas flow around it. The sensor was also pre-calibrated against a reflected shock wave. The initial nitrogen pressure in the driven section was $p_1 = 3.6$ kPa the Mach number of an incident wave was $M_1 = 5.8$, and the expansion ratio of a conical nozzle was 114. The heat flux calculated in accordance with the Fay–Riddell theory [9] and the one-dimensional model of gas flow in a nozzle with account for its real properties was $q_{FR} = 1\,\text{MW/m}^2$. This value was used as a boundary condition in the calculation. As in the previous case, the observed difference between different calculation scenarios is attributable to the structure of the temperature and potential fields. The deviation of calculated signals from the experimental one may be induced by the difference between the one-dimensional calculation of a supersonic gas flow and the actual flow in a nozzle and, consequently, the difference between the experimental heat flux and the one specified as a boundary condition. The indicated differences are also found in the obtained heat flux values (Fig. 2, *d*).

It was demonstrated that the volt–watt coefficient determined in the calculation utilizing a two-dimensional thermal and thermoelectric model, which takes the layered sensor structure into account, deviates by no more than 20% from the experimental one obtained via signal processing with calibration against a reflected shock wave. The calculated and experimental sensor signals agreed closely, which is also true for the calculated and measured heat flux values under heating behind a reflected shock wave and at the critical point of a blunt body with a supersonic flow around it. The obtained results suggest that the used method of heat flux calculation based on the one-dimensional thermal and thermoelectric model allows one to obtain correct results corresponding to various conditions of a gas-dynamic experiment.

Conflict of interest

The author declares that he has no conflict of interest.

References

[1] B.R. Hollis, D.K. Prabhu, M. Maclean, A. Dufrene, J. Thermophys. Heat Transfer, **31** (3), 712 (2017). DOI: 10.2514/1.T5019
[2] S. Gu, H. Olivier, Prog. Aerospace Sci., **113**, 100607 (2020). DOI: 10.1016/j.paerosci.2020.100607
[3] D.R. Buttsworth, Exp. Therm. Fluid Sci., **25** (6), 409 (2001). DOI: 10.1016/S0894-1777(01)00093-0
[4] R.T.P. Geraets, M. McGilvray, L.J. Doherty, R.G. Morgan, C.M. James, D.R. Buttsworth, J. Thermophys. Heat Transfer., **34** (1), 193 (2020). DOI: 10.2514/1.T5688
[5] S.Z. Sapozhnikov, V.Yu. Mityakov, A.V. Mityakov, *Heatmetry. The science and practice of heat flux measurement*. Ser. Heat and Mass Transfer (Springer, Cham, 2020).
[6] D.M. Rowe, *Thermoelectrics handbook: macro to nano* (CRC Press, 2006).
[7] P.A. Popov, N.A. Monakhov, T.A. Lapushkina, S.A. Poniaev, Tech. Phys., **67** (9), 1144 (2022). DOI: 10.21883/TP.2022.09.54677.54-22.
[8] P.A. Popov, N.A. Monakhov, T.A. Lapushkina, S.A. Poniaev, R.O. Kurakin, Tech. Phys. Lett., **48** (10), 46 (2022). DOI: 10.21883/TPL.2022.10.54798.19297.
[9] J.A. Fay, F.R. Riddell, J. Aeronaut. Sci., **25** (2), 73 (1958). DOI: 10.2514/8.7517

Translated by D.Safin